PHYSICAL REVIEW B VOLUME 61, NUMBER 14 1 APRIL 2000-II

Ab initio based modeling of *i*-AlPdMn

Alexander Quandt and Veit Elser
Laboratory of Atomic and Solid State Physics, Ithaca, New York 14853

(Received 20 September 1999)

We discuss a structure model for icosahedral AlPdMn that is based on *ab initio* simulation studies. The main structural features of this model have gradually been refined after studying a series of crystalline reference structures and after optimizing a suitable crystalline approximant for *i*-AlPdMn. We also report on the energetics of possible internal degrees of freedom for the structure model, essentially by performing a line scan of the binding energy as selected atoms are moved within the model approximant. The structure and the decoration of the optimized approximant lead to a set of empirical rules, which apply to the case of the real quasiperiodic structure as well.

I. INTRODUCTION

Despite the fact that *i*-AlPdMn is among the most well-examined quasicrystalline alloy systems, there is still no agreement concerning its basic atomic structure. The six-dimensional (6D) analysis of the corresponding diffraction data appears to be quite simple, as it suggests that atomic positions might be derived from just three relatively compact and flat atomic surfaces.[1] This simple and very appealing result is somewhat flawed by the fact that experimental evidence[2] also suggests an entropic mechanism for the stabilization of *i*-AlPdMn. The simplicity of the atomic surfaces in the entropic scenario would then be the result of the fact that analysis of just the Bragg-diffraction data represents only the *average* atomic structure.[3] Another problem is the incomplete knowledge of chemical segregation in the atomic surfaces[4]; even in the ideal-tiling scenario the chemical identities of many atoms are still uncertain.

A straightforward way to get more information about the atomic structure of quasicrystals is by testing plausible model structures with the help of numerical simulation methods.[5–7] In the past, this kind of approach has not been free from ambiguities either. These arise from shortcuts imposed by the computational cost: pseudobinary treatment of ternary systems, pair-potential energetics, rigid idealized positions. With the increase in computational power and sophistication of algorithms, we can begin to avoid these shortcuts. Current *ab initio* methods allow for the determination of accurate energies and interatomic forces for alloy systems up to about 80–100 atoms (a nice example, which seems to be in good agreement with experimental results, is Ref. 8). By exploring the local chemistry of a quasicrystal approximant with such methods, we can begin to understand in detail the basic chemistry of the quasicrystal, a fact which largely outweighs the somewhat modest size of the model systems. The size of the model in this study, 65 atoms, while small enough to be treated by *ab initio* methods, is very close to being representative of a real quasicrystalline phase constructed from the same building blocks (tiles, clusters).

In the following section, we discuss details of the simulation methods that we used, which should be helpful for other physicists trying to reproduce or extend our results. Next, we report on a series of simulations on a set of elemental and binary reference structures, focusing on those results which turned out to be useful in setting up our model approximant. The next topic is a detailed description of our final version of the atomic structure of the approximant, and the major structural rules it implies. In our discussion we rely on valuable information gained from *ab initio* studies on binary reference systems. The final topic is a discussion of possible internal degrees of freedom. We single out two different atoms that in the ideal geometry have two possible positions within a cage of surrounding atoms. We close with a summary of our main results and suggestions for future work.

II. NUMERICAL DETAILS

All of the numerical simulations were carried out using the VASP *ab initio* package.[8–10] The latter is a density functional[11] (DFT) based *ab initio* code using plane-wave basis sets. The theoretical and practical background for this type of code can be found in Ref. 12.

There are a couple of features that make VASP and related codes especially interesting for the modeling of quasicrystalline structures: First, these codes solve the Kohn-Sham equations[13] on the basis of a preconditioned conjugate gradient procedure,[14] which is reasonably fast and robust even in the case of large intermetallic systems like our approximant (65 atoms). Also, the use of ultrasoft pseudopotentials[15] to represent the ionic cores saves even more memory and computational effort.

Another important general feature is the accuracy of the cohesive energies (usually quoted as binding energy per atom). Reliable energetics can, for example, rule out atomic decorations that seem reasonable from a purely geometrical point of view. Also, the cohesive energies of crystalline reference structures give one a handy estimate for the stability of the model approximant.

Finally, the accuracy of the *ab initio* interatomic forces allows one to perform structural optimizations by relaxing various degrees of freedom such as the shape of the unit cell and the positions of the atoms therein. In our case we used a conjugate gradient type of optimization algorithm,[16] where the line minimizations were carried out with the help of a predictor-corrector procedure using cubic interpolation and Brent's method.[16] The criterion to stop the structural relaxations of the nuclear skeleton and the unit cell of the system

0163-1829/2000/61(14)/9336(9)/$15.00

was a difference in total energy of 10^{-3} eV or better between subsequent steps.

In order to determine the electronic structure for the systems considered within this study, we used as many plane waves in our basis sets as were necessary to avoid wrap-around errors in the fast Fourier subroutines[16] of the code and to have a convergence in the total energy up to an accuracy of about 10^{-3} eV: for the ultrasoft pseudopotentials with core radii 0.983 Å (Al), 1.434 Å (Pd), and 1.323 Å(Mn) used in this study, VASP recommended at least a plane-wave cutoff of 250.00 eV (Al), 198.955 eV (Pd), and 227.24 eV(Mn) to perform qualitatively correct structure optimizations. But in order to arrive at the desired accuracy in the meV region, we generally used a cutoff that was about 30% higher than those recommended values. For example, in the case of the 65-atom model AlPdMn approximant described below, we set the plane-wave cutoff to 312.5 eV.

The criterion for stopping the electronic self-consistent step that solves the Kohn-Sham equations was a difference in total energy of 10^{-4}eV or less between subsequent iterations. In order to determine the occupation of the corresponding bands, we used a smearing method due to Methfessel and Paxton.[17] The smearing factor was chosen such that the error in the corresponding binding energy was around 10^{-3} eV or better. The exchange-correlation functional we used to represent the electronic interactions of the systems was the one suggested by Perdew and Zunger.[18]

In the case of the crystalline reference structures, we used as many k points for sampling in reciprocal space as was necessary to get an error in binding energy of about 10^{-3} eV or better. In the case of the approximant, we were forced to restrict ourselves to just the Γ point, which will certainly be improved in future studies.

III. ENERGETIC STUDY OF CRYSTALLINE REFERENCE STRUCTURES

A rough picture of energetics in our quasicrystal approximant, dominated by pair interations, was formed from a study of simple elementary and binary crystalline phases. In these studies we only relaxed the overall scale (volume) of each structure from that given by diffraction experiments. Errors in the experimentally determined structure parameters are probably negligible so that the scale changes we find are the result of deficiencies in the *ab initio* calculation. Since volume change played a significant role in the relaxation of the approximant, we felt the same relaxation should be applied to the simple crystals in order to allow for a meaningful comparison of binding energies. In general we found that VASP decreased the unit cell volume, although never more than 1% or 2%. This is not so surprising, as it is well known that simulations based on the exchange-correlation functional chosen for this study[18] tend to overbind molecules or solids, which leads, for example, to slightly smaller bond distances than are usually reported in the crystallographic literature.

TABLE I. Crystalline reference structures: Apart from elementary phases (note that fcc-Mn is not the ground state of elementary Mn), we picked a number of reasonably small binary phases as energetic benchmarks.

Substance	Space group	Atoms/unit cell	Coh. energy (eV/atom)
Al	$Fm3m$	1	4.232
Pd	$Fm3m$	1	4.972
Mn	$Fm3m$	1	5.084
$AlPd_2$	$Pnma$	12	5.584
Al_3Pd_5	$Pbam$	16	5.564
AlPd	$Pm3m$	2	5.509
Al_3Pd_2	$P\overline{3}m1$	5	5.342
AlMn	$P4/mmm$	2	4.845
$Al_{11}Mn_4$	$P\overline{1}$	15	4.676
$Al_{10}Mn_3$	$P6_3/mmc$	26	4.651
Al_6Mn	$Cmcm$	28	4.509
PdMn	$Pm3m$	2	4.994
Pd_5Mn_3	$Cmmm$	16	4.714

The results for the cohesive energies of the elementary phases and the binaries are given in Table I. (Readers unfamiliar with the space group notation should consult Ref. 19.) For the elementary phases, we chose the fcc structures of Al, Pd, and Mn. Note that fcc Mn is not the ground state of elementary Mn, which is a complicated cubic system with 58 atoms per unit cell.[20] Crystallographic data describing the elementary phases may be found in Ref. 20 or any of its older editions.

The binary phases chosen from the Al-Pd system comprise CsCl-like PdAl,[21] hexagonal Al_3Pd_2,[21] orthorhombic $AlPd_2$,[22] and orthorhombic Al_3Pd_5.[23] The structural stability of these systems follows from the convexity of the set of pure phases in the energy-composition plane (see Table I). Let us discuss some of their general geometric features, in particular the case of Al_3Pd_2: The Al-Pd bonding distance within this structure was found to be between 2.5 and 2.6 Å and the Al-Al bonding distance was around 2.8 Å. Similar bond lengths were found for all of the other Al-Pd phases considered here. We verified that these are very characteristic bond lengths for the Al-Pd system, by comparing with the structure of the rhombohedral AlPd phase[24] (with 78 atoms per unit cell).

Binary structures chosen from the Al-Mn system were tetragonal AlMn,[25] orthorhombic Al_6Mn,[26] hexagonal $Al_{10}Mn_3$,[27] and triclinic $Al_{11}Mn_4$.[28] The corresponding cohesive energies are listed in Table I. Let us note some of their most prominent geometrical features, focusing on Al_6Mn. Here we found short Al-Al bond distances between 2.5 and 2.6 Å, as well as longer bonds around 2.8 Å. The typical Al-Mn bond distance was between 2.5 and 2.6 Å, but we also found a few bonds around 2.4 Å or even shorter. Similarly short Al-Mn bonds have been reported in the crystallographic literature for $Al_{10}Mn_3$ (Ref. 27) and $Al_{11}Mn_4$.[28]

Finding simple binary phases within the Pd-Mn system turned out to be a real problem. After browsing through the index of the *Structure Reports*[29] and looking up a couple of phases, it became obvious to us that these two elements are better characterized as forming solid solutions.[30] Unfortunately, any *ab initio* simulation of such phases would have been far beyond our means. Among the few phases that we found to be be simple enough for our purposes, we will only mention the CsCl-like PdMn (Ref. 30) and the orthorhombic

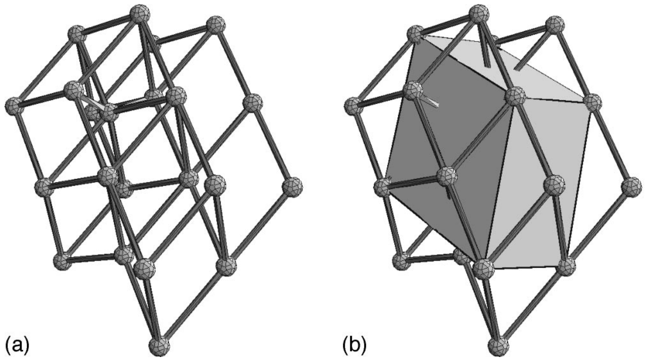

FIG. 1. Geometrical structure of the model approximant. (a) Rhombohedral tiling. (b) Placement of the unit cell within the tiling.

Pd_5Mn_3 phase.[31] Our cohesive energies for these phases (Table I) are not consistent with thermodynamic phase stability. One might of course argue that PdMn should basically be seen as a high-temperature component inside a phase diagram dominated by solid solutions.[30] But also the second phase, Pd_5Mn_3, turned out be unstable with respect to separation into elemental phases. There is, however, an analysis of its interatomic distances published in the literature,[31] which made it worth mentioning here. When comparing our results with the data published in this study, we found that the *ab initio* interatomic distances for Pd_5Mn_3 were shorter than those reported in Ref. 31. Note that the true structure of Pd_5Mn_3 is still the subject of some debate.[31]

Our final conclusion about the PdMn phases was that the disappointing *ab initio* energetics are probably an indication of the fact that direct short bonds between Mn and Pd are somewhat problematic. As we will see below, the cohesive energy of the approximant was generally improved when short Mn-Pd bonds were avoided.

IV. STRUCTURE AND STABILITY OF THE MODEL APPROXIMANT

The process of refining the structure model for the approximant involved two basic parts: (1) constructing an idealized set of sites and candidate chemical occupations and (2) relaxing all degrees of freedom (positions, cell parameters) by *ab initio* structural optimization. These two steps were iterated, with the relaxational data providing clues to improve the selection of sites and chemistry in the next iteration. Our progress was measured by the approximant's cohesive energy (after relaxation) relative to a phase separated mixture of simple crystalline phases. Below we discuss in detail only the structure that was judged ''best'' by this energetic criterion.

A. Geometrical structure

The construction of a suitable model approximant was guided by the fact that the most commonly occuring vertex type in the ideal icosahedral tiling is four coordinated by rhombohedral edges and surrounded by two oblate and two prolate rhombohedra. These oblate and prolate rhombohedra form a rhombic dodecahedron, which tiles space simply by translation, and therefore serves as a convenient approximant for the icosahedral tiling. In Fig. 1, we show a representative part of the rhombohedral tiling together with the unit cell of the model approximant. Two lattice vectors of the approximant, $\vec{a}=(0.000,1.000,0.000)$ and $\vec{b}=(0.618,0.000,0.000)$, are at right angles to each other, whereas the third lattice vector points along $\vec{c}=(0.309,0.5,0.809)$. The overall scale of the lattice vectors is discussed in the next section.

For the atomic decoration of this unit cell, we used the random tiling model[32] as a guide. From Ref. 34 and 6, we knew that the dominant structure elements are the 33-atom Bergman clusters shown in Fig. 2(a). As in Ref. 32, we centered these clusters on alternating (''odd'') vertices of the rhombohedra, thus leading to a network of edge-sharing Bergman clusters, where each cluster shares a pair of atoms with seven surrounding clusters. This determines $2\times33-2\times7=52$ atomic positions within the approximant.

After the placement of the Bergman clusters, the largest empty regions are centered on the ''even'' vertices of the rhombohedra, when these do *not* share the short body diagonal of the oblate rhombohedron with an ''odd'' vertex. This type of void is usually identified as the interior of a Mackay cluster,[32,34] and is usually decorated with a central atom (''M_0'') at the vertex, surrounded by seven atoms distributed among the vertices of a dodecahedron (''M_3''). However, for reasons that will become clear as soon as we discuss the chemistry of these sites, we decided to put a cube, consisting of eight vertices of the dodecahedron, around this central atom, as shown in Fig. 2(b). The orientation of the cube is such that two of its edges are parallel to the lattice vectors $\vec{a}$ and $\vec{b}$. Note that according to the decoration rules given in Ref. 32, any vertex associated with the short body diagonal of an oblate rhombohedral tile is never at the center of a Mackay cluster, while the above-mentioned cube can only be placed at the center of a Mackay cluster. Our approximant has one even vertex not on a short body diagonal, and therefore only one cube.

In addition to the Mackay void, the approximant at this stage contains four smaller voids. Two of them were each filled by a single atom (''P''; see Ref. 32) in a simple fashion; the others correspond to elongated cages of the type sketched in Fig. 2(c). In the model of Katz and Gratias,[34] one of these cages is empty,[35] but we followed the model of Elser[32] and put an atom (''M_2'' or ''M_3'') on one of two equivalent positions inside both cages, as illustrated in Fig. 2(c). The geometrical structures of both cages turn out to be identical. Counting the number of all atomic sites specified by the geometrical decoration rules outlined in this section, we finally end up with $52+1+8+2+2=65$ atoms.

B. Chemistry

Experimental facts which guided our choices in chemical occupations of the 65 sites were the composition of the icosahedral phase, the results of anomalous x-ray scattering experiments,[4] which limits the possible Pd sites, and the spherical chemical segregation in the 6D model of Boudard *et al.*[1]. The anomalous x-ray scattering showed that the ''odd'' rhombohedral vertices were occupied by Pd,[4] and the spherical model suggests that Mn atoms occupy the remaining rhombohedral vertices, as well as the *P*-type sites mentioned above.[1] Most of our remaining choices were then decided by *ab initio* simulations.

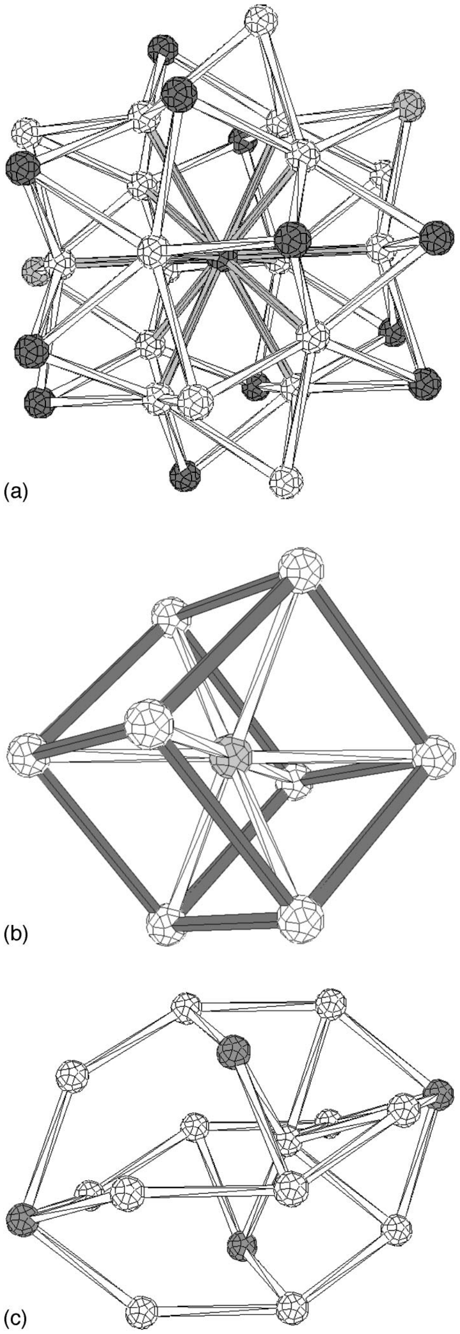

FIG. 2. Details of the ideal structure: (a) Decorated Bergman cluster, (b) cube around Mn atom, (c) interstitial cage. The darkest balls correspond to Pd, lighter balls correspond to Mn, and the white balls correspond to Al. Similarly, the darkest bonds are along twofold axes, lighter bonds are along fivefold axes, and the white bonds are all along threefold axes.

As we described above, the majority of all atomic positions of the model are part of Bergman clusters, where we find three kinds of near-neighbor separations (‘‘bonds’’), corresponding to ‘‘threefold,’’ ‘‘fivefold,’’ and ‘‘twofold’’ axes of the icosahedron. From the lattice constant of the icosahedral phase, these have ‘‘ideal’’ lengths given by 2.57 Å (threefold), 2.82 Å (fivefold), and 2.96 Å (twofold). From studies of the simple binaries we concluded that the short threefold bonds always involved one Al and one transition metal. When this rule was broken (see below) we invariably found large distortions from the ideal geometry upon relaxation. In the ideal geometry specified by twofold, threefold, and fivefold bonds, the unit cell parameters of our approximant are $\vec{a}=(0,12.555,0)$, $\vec{b}=(7.758,0,0)$, and $\vec{c}=(3.879,6.277,10.157)$ in units of 1 Å. This corresponds to a cell volume of 989.44 $Å^3$.

An example of how *ab initio* calculations provided clues to the chemistry is the case of the icosahedral shell of sites surrounding the central Pd in the Bergman cluster. We first tried the 9Al+3Mn arrangement arrived at in Ref. 6 for an AlCuFe approximant. Apparently the Mn and Pd atoms at this fivefold separation are much too close because the relaxations distorted the structure, so as to move these atoms away from each other. Together with the anomalous x-ray data, this left no choice but to occupy all 12 sites with Al. A similar effect occurs within the Mackay void, where we ended up occupying all 8 sites of the cube surrounding Mn by Al. This makes the cube rather similar to local features within the stable tetragonal phase AlMn.[25] More generally, we avoided any transition-metal-to-transition-metal contacts shorter than the twofold bond.

The typical coordinations along threefold bonds (and some fivefold bonds) for the various atoms of the model approximant are shown in Fig. 3. Note that the real coordination up to 3.0 Å is somewhat higher (including *all* threefold, fivefold, and twofold bonds), and it ranges form 9 (some Mn) to 13 (some Al). It is obvious from Fig. 3 that the transition metals in the approximant tended to occupy sites where they have the largest number of threefold bonds [or fivefold bonds in the special case of Fig. 3(g)], always to Al. The resulting decoration of the network of threefold bonds leads to the atomic decoration of the major structure elements shown in Fig. 2. One fact worth mentioning here is that the final decorations of the two elongated cages inside the model approximant turned out to be identical even from a chemical point of view. The coordinates for the ideal approximant are given in the Appendix.

C. Optimized structure model

The resulting chemical composition of our approximant ($Al_{46}Pd_{14}Mn_5$) lies within the triangle of compositions Al, $Al_{11}Mn_4$, and Al_3Pd_2 in the Al-Pd-Mn plane. Phase separation into these phases implies a cohesive energy of 4.958 eV/atom (see Table I). These numbers should be compared to the final cohesive energy of our approximant : 4.894 eV/atom (4.748 eV/atom before relaxation).

If the VASP energies (or rather energy differences) are correct, then we must conclude that our approximant is *not* stable to phase separation. This is not in itself a problem, since there are no indications experimentally of an approximant phase in the Al-Pd-Mn phase diagram having a size as small as our 65-atom model. On the other hand, the energy difference, 0.064 eV/atom, is too large to be accounted for by an entropic contribution in the icosahedral phase (and absent in the approximant). At 1000 K this would correspond to roughly an entropy of log 2 per atom. A more likely interpretation is that our approximant is too small to be truly representative of the icosahedral phase. For example, the ratio of prolate to oblate rhombohedra in the icosahedral phase (ideal or random tiling) is τ:1, but only 1 : 1 in our approx-

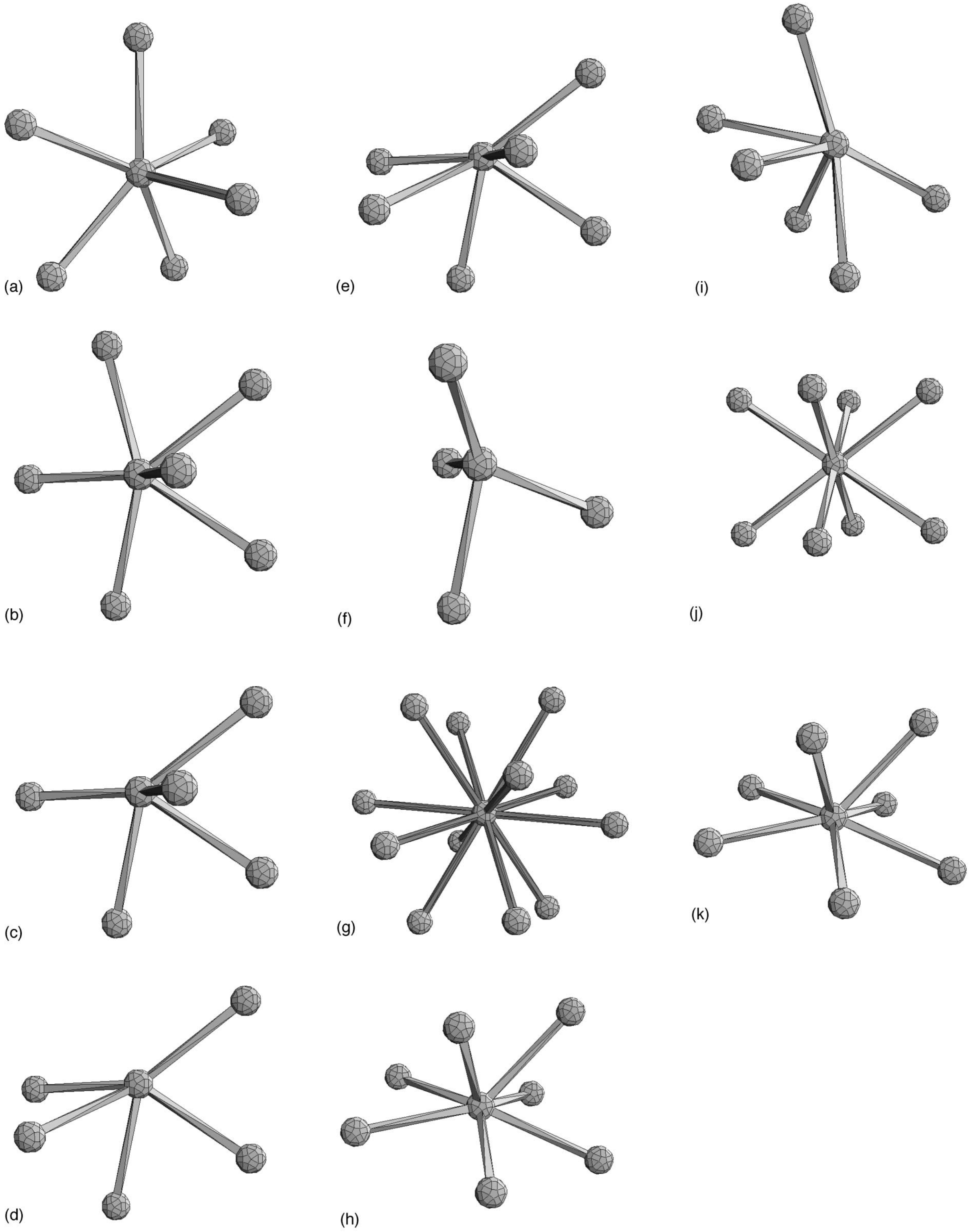

FIG. 3. Sketch of typical bond configurations: (a)-(f) correspond to Al atoms, (g)-(i) correspond to Pd atoms, and (j) and (k) correspond to Mn atoms. Note that the real coordination is somewhat higher (see text); only threefold bonds and fivefold bonds [in (g) and one in (a)] are shown.

imant. With a higher concentration of prolate rhombohedra in the *i* phase, we have a correspondingly higher concentration of ‘‘*P*’’ atoms (Mn), and expect an improvement in cohesive energy due to close Al-Mn contacts.

Independent of its energetic viability, the relaxation of our approximant brings into focus the validity of modeling icosahedral structures as networks of ideal twofold, threefold, and fivefold bonds. With the exception of two atoms, and an overall volume change (from 989.44 Å^3 to 946.33 Å^3), we found that the displacements of atoms from idealized positions are indeed very small. When the relaxed positions were rescaled to restore the original lattice parameters they were

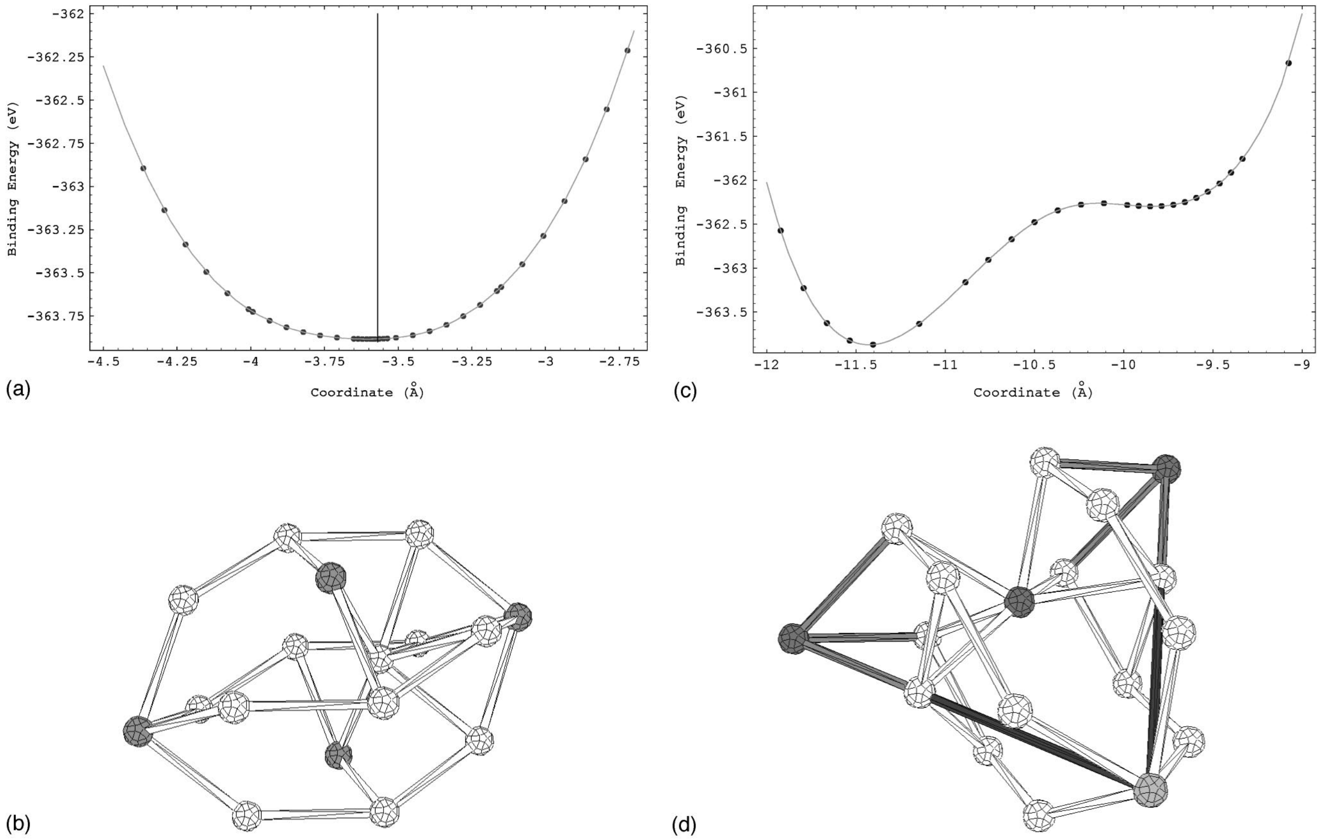

FIG. 4. Internal degrees of freedom: (a) Energetics of a line scan (binding energy in eV/atom vs distance in Å) for the (b) Al atom number 25 (see Appendix) moving along a twofold axis through the middle of one of the cages. (c) Line scan for the hypothetical jump of the Pd atom number 49 (see Appendix) originally shared by two Bergman clusters along a twofold axis towards the interior of the Mackay cluster. Note that the shading of the atoms (d) corresponds to the shading described in Fig. 2. The white bonds correspond to threefold bonds, while the dark bonds (and axes) correspond to fivefold bonds (tile edges) connecting Bergman and Mackay cluster centers.

found to deviate from the original positions by less than 0.2 Å on the average. The two exceptional atoms are Al inside the elongated cages [Fig. 2(c)]. Not surprisingly, these atoms move to the centers of their cages, away from the off-center ideal positions. A complete list of coordinates for the relaxed structure is given in the Appendix.

V. INTERNAL DEGREES OF FREEDOM

There are two situations in our approximant where atoms reside in an elongated cage, containing two ideal positions. The first is the cage shown in Fig. 2(c), which contains an Al atom at its center. As mentioned in Sec. IV two such cages, at right angles to each other, occur in the approximant. The second situation involves a cage which is identical in geometry, but differs significantly in chemistry [Fig. 4(b)]. This ‘‘cage’’ was not identified as such in our earlier discussion because structurally it made more sense to identify its parts with Bergman clusters and the interior of the Mackay cluster. The atom in the cage interior is Pd, which is shared by two Bergman clusters when it sits at one of the off-center ideal sites. Although virtually identical in geometrical structure, our *ab initio* calculations show that these cage atoms have very different energetics. To this end, we carried out two line scans, which examined the changes in the binding energy when an atom was moved along a selected direction, while keeping all other atoms of the approximant frozen. The line scan obtained when the Al atom number 25 (see the Appendix) is moved on the axis of its cage [Fig. 4(a)] shows a broad minimum at the center of the cage (or just slightly displaced from the center for the cage which is asymmetrically distorted by its environment). In contrast, the line scan for the Pd atom number 49 (see the Appendix) shows that this cage atom clearly prefers the off-center ideal site that maintains the integrity of the Bergman clusters. This scan also shows a very shallow minimum near the other ideal position, but this is higher in energy by 1.57 eV.

The two elongated cages containing Al atoms are reasonable candidates for quasilocalized phonon modes. The broad minimum in the line scan shown in Fig. 4(a) implies that the central Al atom will have a much larger displacement than the surrounding cage atoms. A good estimate of the frequency of this mode is therefore just the Einstein frequency of an Al atom subject to the 1D potential given by the line scan:

$$V(x)=\frac{1}{2}\kappa(x-x_0)^2, \tag{1}$$

where x_0 is the position of minimal energy. Fitting κ to points near the minimum, we find $\kappa=1.5$ eV/Å^2 and an oscillator frequency

TABLE II. Fractional coordinates (x,y,z) of the idealized approximant structure. The Cartesian atomic coordinates are obtained from $\vec{r}=x\vec{a}+y\vec{b}+z\vec{c}$, where the Cartesian basis vectors are $\vec{a}=(0.00000,12.555400,0.000000)$, $\vec{b}=(7.758421,0.000000,0.000000)$, and $\vec{c}=(3.879832,6.277700,10.157519)$ in units of 1 Å.

No.	Type	x	y	z	No.	Type	x	y	z
1	Al	0.881966	0.072949	0.854102	34	Al	0.263932	0.690983	0.236068
2	Al	0.736068	0.927051	0.145898	35	Al	0.072949	0.190983	0.236068
3	Al	0.263932	0.072949	0.854102	36	Al	0.927051	0.045085	0.527864
4	Al	0.118034	0.927051	0.145898	37	Al	0.072949	0.572949	0.236068
5	Al	0.118034	0.927051	0.763932	38	Al	0.927051	0.427051	0.527864
6	Al	0.881966	0.690983	0.236068	39	Al	0.690983	0.190983	0.236068
7	Al	0.881966	0.690983	0.000000	40	Al	0.545085	0.045085	0.527864
8	Al	0.118034	0.690983	0.000000	41	Al	0.309017	0.427051	0.145898
9	Al	0.881966	0.309017	0.000000	42	Al	0.072949	0.190983	0.618034
10	Al	0.118034	0.309017	0.000000	43	Al	0.545085	0.427051	0.145898
11	Al	0.118034	0.309017	0.763932	44	Al	0.309017	0.190983	0.618034
12	Al	0.881966	0.072949	0.236068	45	Al	0.690983	0.572949	0.236068
13	Al	0.500000	0.690983	0.618034	46	Al	0.545085	0.427051	0.527864
14	Al	0.354102	0.545085	0.909830	47	Pd	0.545085	0.045085	0.909830
15	Al	0.881966	0.690983	0.618034	48	Pd	0.072949	0.572949	0.854102
16	Al	0.736068	0.545085	0.909830	49	Pd	0.690983	0.809017	0.381966
17	Al	0.736068	0.545085	0.527864	50	Pd	0.927051	0.809017	0.381966
18	Al	0.500000	0.309017	0.000000	51	Pd	0.309017	0.190983	0.000000
19	Al	0.500000	0.309017	0.763932	52	Pd	0.690983	0.190983	0.000000
20	Al	0.736068	0.309017	0.763932	53	Pd	0.309017	0.809017	0.000000
21	Al	0.500000	0.927051	0.763932	54	Pd	0.690983	0.809017	0.000000
22	Al	0.736068	0.927051	0.763932	55	Pd	0.309017	0.427051	0.763932
23	Al	0.736068	0.927051	0.527864	56	Pd	0.927051	0.427051	0.763932
24	Al	0.500000	0.690983	0.000000	57	Pd	0.309017	0.809017	0.763932
25	Al	0.309017	0.427051	0.381966	58	Pd	0.927051	0.809017	0.763932
26	Al	0.736068	0.309017	0.381966	59	Pd	0.000000	0.000000	0.000000
27	Al	0.263932	0.072949	0.236068	60	Pd	0.618034	0.618034	0.763932
28	Al	0.118034	0.927051	0.527864	61	Mn	0.500000	0.309017	0.381966
29	Al	0.500000	0.072949	0.236068	62	Mn	0.118034	0.309017	0.381966
30	Al	0.354102	0.927051	0.527864	63	Mn	0.927051	0.427051	0.145898
31	Al	0.354102	0.545085	0.527864	64	Mn	0.690983	0.190983	0.618034
32	Al	0.500000	0.690983	0.236068	65	Mn	0.309017	0.809017	0.381966
33	Al	0.118034	0.545085	0.527864					

$$\omega=\sqrt{\frac{\kappa}{M_{\mathrm{Al}}}}=2.32\times 10^{13}\ \ s^{-1}=0.096\ \ \mathrm{eV}=1110\ \ \mathrm{K}, \tag{2}$$

with M_{Al} being the atomic mass of Al. The density of such modes, 2/65 atom, should have a similar value in the icosahedral phase and polarization along two-fold axes.

VI. SUMMARY

We have studied the structure and chemistry of *i*-AlPdMn using *ab initio* simulation methods. After presenting a number of binary reference structures, we described what we learned about their stability and made some observations about their chemistry. This information, in combination with earlier structural studies of *i*-AlPdMn,[1,32–34] led us to the construction of a 65-atom model approximant of composition $Al_{46}Pd_{15}Mn_5$. Here, *ab initio* simulation methods were useful in working out an optimal decoration that was in agreement with experimental results[4] and the basic chemical rules we determined from our studies of the reference structures. The dominant structural element of this model is a network of *Bergman clusters* [see Fig. 2(a)], with Pd centers and an inner icosahedral shell composed of 12 Al atoms, centered around alternating (''odd'') vertices of a rhombohedral tiling. On some of the remaining (''even'') vertices, there are Mn atoms, eventually surrounded by an 8-atom *cube* of Al atoms [see Fig. 2(b)], forming the center of a Mackay cluster. The remaining atoms are second shell Bergman atoms (Al,Pd,Mn), ''*P*'' atoms (Mn),[1] and Al atoms located inside elongated cages [see Fig. 2(c)].

The atomic decoration of the model follows a number of empirically determined rules: First, the shortest (threefold) bonds always involve one Al atom and one transition metal atom, such that the transition metals have the largest number of Al binding partners along threefold axes. Second, the shortest allowed separation of transition metals (Mn-Pd and

Pd-Pd) is the twofold bond (2.96 Å). We found that it is indeed possible to construct a decoration subject to all of these constraints. Part of the decoration can be inferred from Fig. 2. It turned out that the relaxation of the idealized approximant led to only very slight structural distortions. The dominant processes were a noticeable shrinking of the unit cell and the movement of two Al atoms toward the centers of cages [see Fig. 2(c)]. We decided to examine this movement in more detail, together with a Pd atom which inhabits a cage that is identical geometrically, but different chemically. We found that the Al atoms behave like a localized mode while the Pd atom prefers the off-center site that preserves the second shell of a pair of Bergman clusters. The cohesive energy of our approximant is short, by 0.064 eV/atom, of being stable to phase separation into simpler crystalline phases. This value is small, and might be remedied in a larger approximant which has a larger fraction of the prolate rhombohedral tile.

ACKNOWLEDGMENTS

The authors would like to thank the Deutsche Forschungsgemeinschaft (DFG) for financial support under the Project No. Qu 119/1-1. We also thank M.P. Teter (Cornell), M. Mihalkovic (Chemnitz), and D. Joseph (Dresden) for numerous helpful suggestions during all stages of this project. Finally we would like to thank G. Kresse (Wien), B. Robinson, and J. Neaton (Cornell) for their patience and continuous support during the time of our extensive usage of the VASP package at LASSP, Cornell.

APPENDIX: STRUCTURAL DETAILS AND COORDINATES.

This appendix lists the structural data of the idealized approximant as well as of the relaxed approximant discussed in

TABLE III. Fractional coordinates (x,y,z) of the relaxed approximant structure. The Cartesian atomic coordinates are obtained from $\vec{r}=x\vec{a}+y\vec{b}+z\vec{c}$, where the Cartesian basis vectors are $\vec{a}=(-0.000020, 12.945323, 0.000377)$, $\vec{b}=(7.1382411,-0.000140,-0.000192)$, and $\vec{c}=(3.569433, 6.472886, 10.242350)$ in units of 1 Å.

No.	Type	x	y	z	No.	Type	x	y	z
1	Al	0.877276	0.064264	0.873747	34	Al	0.259693	0.685453	0.253971
2	Al	0.746920	0.930309	0.138184	35	Al	0.055768	0.191565	0.258149
3	Al	0.247327	0.064456	0.873335	36	Al	0.931937	0.067783	0.505767
4	Al	0.113135	0.930342	0.138078	37	Al	0.052269	0.547465	0.258591
5	Al	0.121939	0.936034	0.754025	38	Al	0.928885	0.424077	0.505354
6	Al	0.888874	0.706950	0.219954	39	Al	0.683323	0.191462	0.258063
7	Al	0.885253	0.692692	0.999504	40	Al	0.559340	0.067510	0.505908
8	Al	0.113554	0.692861	0.999452	41	Al	0.277529	0.431990	0.141652
9	Al	0.885408	0.308469	0.000701	42	Al	0.037235	0.191672	0.622261
10	Al	0.112185	0.308335	0.000655	43	Al	0.577881	0.431910	0.141885
11	Al	0.121240	0.311440	0.755401	44	Al	0.337742	0.191825	0.622060
12	Al	0.888093	0.076589	0.221491	45	Al	0.686403	0.547669	0.258505
13	Al	0.503152	0.686515	0.625748	46	Al	0.562888	0.424196	0.505458
14	Al	0.369049	0.556047	0.890176	47	Pd	0.547586	0.049826	0.903276
15	Al	0.869251	0.686473	0.625849	48	Pd	0.068900	0.571127	0.860664
16	Al	0.738676	0.555833	0.890586	49	Pd	0.691810	0.810101	0.381975
17	Al	0.726857	0.544973	0.543965	50	Pd	0.923966	0.810116	0.381960
18	Al	0.494003	0.308098	0.009918	51	Pd	0.297889	0.198084	0.014724
19	Al	0.502794	0.310235	0.764434	52	Pd	0.685263	0.197861	0.015418
20	Al	0.731049	0.310342	0.764508	53	Pd	0.300016	0.792184	0.011897
21	Al	0.504151	0.927195	0.763236	54	Pd	0.685976	0.791751	0.012558
22	Al	0.730885	0.927013	0.763304	55	Pd	0.316596	0.422352	0.751335
23	Al	0.727602	0.916104	0.542440	56	Pd	0.929963	0.422132	0.752000
24	Al	0.494677	0.684863	0.008545	57	Pd	0.318746	0.831343	0.748458
25	Al	0.307560	0.336904	0.381959	58	Pd	0.930648	0.830833	0.749207
26	Al	0.807615	0.310948	0.381934	59	Pd	0.003924	0.004985	0.990394
27	Al	0.263454	0.070056	0.256751	60	Pd	0.612340	0.613400	0.773552
28	Al	0.138223	0.944829	0.507179	61	Mn	0.490754	0.310640	0.381978
29	Al	0.476856	0.070079	0.256775	62	Mn	0.124670	0.310664	0.381950
30	Al	0.351640	0.944897	0.507152	63	Mn	0.924892	0.427431	0.148497
31	Al	0.355434	0.557574	0.509955	64	Mn	0.691486	0.193966	0.615459
32	Al	0.483444	0.685575	0.253965	65	Mn	0.307545	0.805971	0.381954
33	Al	0.131685	0.557464	0.509971					

Sec. IV. When the inner Al atoms of the two cages sketched in Fig. 2(c) are located exactly in the center of their cages, the space group is $I2/m\ 2/m\ 2/m$ (orthorhombic). The Cartesian coordinates of the basis vectors $\vec{a},\vec{b}$, and $\vec{c}$, and the fractional atomic coordinates (x,y,z) relative to this basis, are printed in Table II for the idealized approximant, and in Table III for the relaxed approximant. Important points of reference for both structures are the atoms 25 and 26, which are the inner Al atoms of the cages, the atoms 59 and 60, which mark the centers of the two Bergman clusters, and the atom 65, which marks the center of both the Mackay cluster and the cube.

---

[1] M. Boudard, M. de Boissieu, C. Janot, G. Heger, C. Beeli, H.-U. Nissen, H. Vincent, R. Iberson, R. Audier, and J.M. Dubois, J. Phys.: Condens. Matter **4**, 10149 (1992).

[2] M. de Boissieu, M. Boudard, B. Hennion, R. Bellissent, S. Kycia, A. Goldman, C. Janot, and M. Audier, Phys. Rev. Lett. **75**, 89 (1995).

[3] C. L. Henley, *Quasicrystals: The State of the Art*, edited by D. P. DiVincenzo and P. J. Steinhardt (World Scientific, Singapore, 1991), p. 429.

[4] M. de Boissieu, P. Stephens, M. Boudard, C. Janot, D.L. Chapman, and M. Audier, Phys. Rev. Lett. **72**, 3538 (1994).

[5] M. Mihalkovic, W.-J. Zhu, C.L. Henley, and M. Oxborrow, Phys. Rev. B **53**, 9002 (1996).

[6] E. Cockayne, R. Phillips, X.B. Kan, S.C. Moss, J.L. Robertson, T. Ishimasa, and M. Mori, J. Non-Cryst. Solids **153-154**, 140 (1993).

[7] E. Cockayne and M. Widom, Phys. Rev. Lett. **81**, 598 (1998).

[8] M. Krajcí, M. Windisch, J. Hafner, G. Kresse, and M. Mihalkovic, Phys. Rev. B **51**, 17 355 (1995).

[9] G. Kresse and J. Furthmüller, Comput. Mater. Sci. **6**, 15 (1996).

[10] G. Kresse and J. Furthmüller, Phys. Rev. B **54**, 11 169 (1996).

[11] P. Hohenberg and W. Kohn, Phys. Rev. **136**, 864 (1964).

[12] M.C. Payne, M.P. Teter, D.C. Allan, T. Arias, and J.D. Joannopoulos, Rev. Mod. Phys. **64**, 1045 (1992).

[13] W. Kohn and L.J. Sham, Phys. Rev. **140**, 1133 (1965).

[14] M.P. Teter, M.C. Payne, and D.C. Allan, Phys. Rev. B **40**, 12 255 (1989).

[15] D. Vanderbilt, Phys. Rev. B **41**, 7892 (1990).

[16] W. H. Press, S. A. Teukolsky, W. T. Vetterling, and B. P. Flannery, *Numerical Recipes* (Cambridge University Press, New York, 1996).

[17] M. Methfessel and A.T. Paxton, Phys. Rev. B **40**, 3616 (1989).

[18] J. Perdew and A. Zunger, Phys. Rev. B **23**, 5048 (1982).

[19] *International Tables for Crystallography*, edited by T. Hahn (Kluwer Academic, Dordrecht, 1996).

[20] *Metals Reference Book*, by C. J. Smithellsd (Butterworths, Boston, 1992).

[21] J.P. Simanov, Zh. Fiz. Khim. **27**, 1503 (1953).

[22] L.E. Edshammar and V. Björnstjerna, Acta Chem. Scand. **17**, 1803 (1963).

[23] *Structure Reports*, edited by W. B. Pearson (Kluwer Academic, Dordrecht, 1959), Vol. 23, p.121.

[24] T. Matkovic and K. Schubert, J. Less-Common, J. Less-Common Met. **55**, 45 (1977).

[25] P.B. Braun and J.A. Goedkoop, Acta Crystallogr. **16**, 737 (1963).

[26] A. Kontio and P. Coppens, Acta Crystallogr., Sect. B: Struct. Crystallogr. Cryst. Chem. **37**, 433 (1981).

[27] M.A. Taylor, Acta Crystallogr. **12**, 393 (1959).

[28] A. Kontio, E.D. Stevens, P. Coppens, R.D. Brown, A.E. Dwight, and J.M. Williams, Acta Crystallogr., Sect. B: Struct. Crystallogr. Cryst. Chem. **36**, 435 (1980).

[29] *Structure Reports (Index)*, edited by G. Ferguson (Kluwer Academic, Dordrecht, 1990).

[30] E. Raub and W. Mahler, Z. Metallkd. **45**, 430 (1954).

[31] G. Kadar and E. Kren, Solid State Commun. **11**, 933 (1972).

[32] V. Elser, Philos. Mag. B **73**, 641 (1996).

[33] V. Elser, in *Proceedings of the 6th International Conference on Quasicrystals*, edited by S. Takeuchi and T. Fujiwara (World Scientific, Singapore, 1998), p.19.

[34] A. Katz and D. Gratias, J. Non-Cryst. Solids **153-154**, 187 (1993).

[35] Z. Papadopolos, P. Kramer, and W. Liebermeister, in *Proceedings of the International Conference on Aperiodic Crystals ’97*, edited by M. de Boissieu, J. L. Verger-Gaugry, and R. Currat (World Scientific, Singapore, 1998), p. 173.